Layer-by-layer self-assembly of plexcitonic nanoparticles

Brendan G. DeLacy,[1,*] Wenjun Qiu[2], Marin Soljačić,[2] Chia Wei Hsu,[2] Owen D. Miller,[3] Steven G. Johnson,[3] and John D. Joannopoulos[2]

[1]*U.S. Army Edgewood Chemical Biological Center, Research & Technology Directorate 5183 Blackhawk Rd., Aberdeen Proving Ground, MD 21010-5424, USA*
[2]*Department of Physics, Massachusetts Institute of Technology 77 Massachusetts Ave, Cambridge, MA 02139, USA*
[3]*Department of Mathematics, Massachusetts Institute of Technology 77 Massachusetts Ave, Cambridge, MA 02139, USA*
* brendan.g.delacy.civ@mail.mil

Abstract: Colloidal suspensions of multilayer nanoparticles composed of a silver core, a polyelectrolyte spacer layer (inner shell), and a J-aggregate cyanine dye outer shell have been prepared for the first time. Absorption properties of the colloid were measured in the visible region. This multilayer architecture served as a framework for examining the coupling of the localized surface plasmon resonance exhibited by the silver core with the molecular exciton exhibited by the J-aggregate outer shell. The polyelectrolyte spacer layer promotes the formation of an excitonic J-aggregate while serving as a means of controlling the plasmon-exciton (i.e. plexciton) coupling strength through changing the distance between the core and the shell. An analytical expression based on Mie Theory and the Transfer Matrix Method was obtained for describing the optical response of these multilayered nanostructures. Computational and experimental results indicate that the absorption wavelength of the J-aggregate form of the dye is dependent on both the distance of the dye layer from the silver core and the degree of dye aggregation.

References and links

1. M. Kerker, *The Scattering of Light and Other Electromagnetic Radiation* (Academic Press, 1969).
2. S. A. Maier, *Plasmonics: Fundamentals and Applications* (Springer, 2010).
3. C. Noguez, "Surface plasmons on metal nanoparticles: the influence of shape and physical environment," J. Phys. Chem. C **111**(10), 3806–3819 (2007).
4. H. Wang, D. W. Brandl, P. Nordlander, and N. J. Halas, "Plasmonic nanostructures: artificial molecules," Acc. Chem. Res. **40**(1), 53–62 (2007).
5. K. Kneipp, H. Kneipp, I. Itzkan, R. R. Dasari, and M. S. Feld, "Ultrasensitive chemical analysis by Raman spectroscopy," Chem. Rev. **99**(10), 2957–2976 (1999).
6. J. R. Lakowicz, "Radiative decay engineering 5: metal-enhanced fluorescence and plasmon emission," Anal. Biochem. **337**(2), 171–194 (2005).
7. P. J. Chakraborty, "Metal nanoclusters in glasses as nonlinear photonic materials," J. Mater. Sci. **33**(9), 2235–2249 (1998).
8. T. Tani, *Photographic Sensitivity*, (Oxford University, 1995).
9. F. Würthner, T. E. Kaiser, and C. R. Saha-Möller, "J-Aggregates: from serendipitous discovery to supramolecular engineering of functional dye materials," Angew. Chem. Int. Ed. Engl. **50**(15), 3376–3410 (2011).
10. A. S. Davydov, *Theory of Molecular Excitons* (Plenum, 1971).
11. M. van Burgel, D. A. Wiersma, and K. Duppen, "The dynamics of one-dimensional excitons in liquids," J. Chem. Phys. **102**(1), 20–33 (1995).
12. J. Hranisavljevic, N. M. Dimitrijevic, G. A. Wurtz, and G. P. Wiederrecht, "Photoinduced charge separation reactions of j-aggregates coated on silver nanoparticles," J. Am. Chem. Soc. **124**(17), 4536–4537 (2002).

13. G. A. Wurtz, P. R. Evans, W. Hendren, R. Atkinson, W. Dickson, R. J. Pollard, A. V. Zayats, W. Harrison, and C. Bower, "Molecular plasmonics with tunable exciton-plasmon coupling strength in J-aggregate hybridized Au nanorod assemblies," Nano Lett. **7**(5), 1297–1303 (2007).
14. N. Kometani, M. Tsubonishi, T. Fujita, K. Asami, and Y. Yonezawa, "Preparation and optical absorption spectra of dye-coated Au, Ag, and Au/Ag colloidal Na noparticles in aqueous solutions and in alternate assemblies," Langmuir **17**(3), 578–580 (2001).
15. N. T. Fofang, T. H. Park, O. Neumann, N. A. Mirin, P. Nordlander, and N. J. Halas, "Plexcitonic nanoparticles: Plasmon-exciton coupling in nanoshell-j-aggregate complexes," Nano Lett. **8**(10), 3481–3487 (2008).
16. A. Yoshida, Y. Yonezawa, and N. Kometani, "Tuning of the spectroscopic properties of composite nanoparticles by the insertion of a spacer layer: effect of exciton-plasmon coupling," Langmuir **25**(12), 6683–6689 (2009).
17. P. C. Lee and D. Meisel, "Adsorption and surface-enhanced Raman dyes on silver and gold sols," J. Phys. Chem. **86**(17), 3391–3395 (1982).
18. B. D. Busbee, S. O. Obare, and C. Murphy, "An improved synthesis of high-aspect-ratio gold nanorods," J. Adv. Mater. **15**(5), 414–416 (2003).
19. Q. Zhang, N. Li, J. Goebl, Z. Lu, and Y. Yin, "A Systematic Study of the Synthesis of Silver Nanoplates: Is Citrate a "Magic" Reagent?" J. Am. Chem. Soc. **133**(46), 18931–18939 (2011).
20. N. R. Jana, L. Gearheart, and C. J. Murphy, "Wet chemical synthesis of silver nanorods and nanowires of controllable aspect ratio," Chem. Commun. (Camb.) **0**(7), 617–618 (2001).
21. G. B. Sukhorukov, E. Donath, H. Lichtenfel, E. Knippel, M. Knippel, A. Budde, and H. Möhwald, "Layer-by-layer self assembly of polyelectrolytes on colloidal particles," Coll. and Surf. A: Phys. and Eng. Aspects **137**(1-3), 253–266 (1998).
22. G. B. Sukhorukov, E. Donath, S. Davis, H. Lichtenfeld, F. Caruso, V. I. Popov, and H. Möhwald, "Stepwise polyelectrolyte assembly on particle surfaces: a novel approach to colloid design," Polym. Adv. Technol. **9**(10-11), 759–767 (1998).
23. W. Qiu, B. G. DeLacy, S. G. Johnson, J. D. Joannopoulos, and M. Soljačić, "Optimization of broadband optical response of multilayer nanospheres," Opt. Express **20**(16), 18494–18504 (2012).
24. H. C. van de Hulst, *Light Scattering by Small Particles*, (Dover, 1981).
25. C. Bohren and D. Huffman, *Absorption and Scattering of Light by Small Particles*, (John Wiley & Sons,1983).
26. R. E. Hamam, A. Karalis, J. D. Joannopoulos, and M. Soljačić, "Coupled-mode theory for general free-space resonant scattering of waves," Phys. Rev. A **75**(5), 053801 (2007).
27. Z. Ruan and S. Fan, "Superscattering of light from subwavelength nanostructures," Phys. Rev. Lett. **105**(1), 013901 (2010).
28. Z. Ruan and S. Fan, "Temporal coupled-mode theory for fano resonance in light scattering by a single obstacle," J. Phys. Chem. C **114**(16), 7324–7329 (2010).
29. Z. Ruan and S. Fan, "Design of subwavelength superscattering nanospheres," Appl. Phys. Lett. **98**(4), 043101 (2011).
30. T. Kobayashi, *J-Aggregates*, (World Scientific Publishing Co. Pte. Ltd., 1996).
31. A. Dixon, C. Duncan, and H. Samha, "Self assembly of cyanine dye on clay nanoparticles," Am. J. Undergrad. Res. **3**, 29–34 (2005).
32. H. Kuhn and H. D. Foresterling, *Principles of Physical Chemistry* (Wiley, 2000).
33. E. D. Palik, *Handbook of Optical Constants of Solids* (Academic, 1985).
34. Y. Zong, F. Xu, X. Su, and W. Knoll, "Quartz crystal microbalance with integrated surface plasmon grating coupler," Anal. Chem. **80**(13), 5246–5250 (2008).

1. Introduction

Silver and gold nanoparticles have been studied extensively for their unique optical properties in the UV, visible, and infrared regions of the electromagnetic spectrum [1–4]. These properties arise from the collective oscillation of conduction band electrons throughout the particle in response to optical excitation, a process commonly termed as localized surface plasmon resonance. Resonance occurs when the frequency of incident radiation is at or near the frequency of the electronic oscillation. This resonance results in a strong enhancement of the local electric field, useful for surface-enhanced Raman scattering (SERS), surface-enhanced fluorescence, and the study of nonlinear optical response [5–7]. Additionally, the size and morphology of the silver and gold nanoparticles have a significant impact on surface plasmon resonance frequency and therefore have a great significance in such fields as sensors and photonic devices.

Cyanine dyes are commonly used in spectral sensitization, and have potential application in novel optoelectronic materials [8]. Structurally, these dyes consist of two heterocyclic units that are connected by an odd number of methine groups $(CH)_n$ (n = 1,3,5, etc.). The color of the dye is mainly determined by the length of the polymethine chain [9]. A particularly

intriguing property of cyanine dyes is their tendency to aggregate under certain conditions in solution. These so called J-aggregates exhibit a narrow absorption band that is red shifted with respect to the monomer absorption band [9]. The shift in absorption of the aggregate has been described by a Frenkel exciton model, in which excited states are formed by the coherent coupling of molecular transition dipoles [10,11].

Multi-layered nanoparticles, composed of both a noble metal and a J-aggregate dye, provide a unique framework for studying plasmon-exciton interactions. Numerous structures exhibiting these plasmon-exciton interactions have been fabricated and studied in recent years. Some nanostructures have involved the direct adsorption of J-aggregate dyes onto the surface of silver nanoparticles with varying geometries [12–14]. Other efforts have focused on the aggregation of cyanine dyes onto complex geometries. For example, cyanine dyes were adsorbed onto silica core/gold shell nanoparticles [15]. In these studies, it was observed that the absorption spectra of these composite nanoparticles were not the simple sum of the absorption of the metal nanoparticle and the J-band of the aggregate. Rather, strong plasmon-exciton interactions (plexcitons) were observed, resulting in a shift in the absorption bands of the individual plasmon and exciton resonances. A more recent study by Yoshida et al. explored the impact of inserting a spacer layer (inner shell) between a metallic core particle (Au) and an outer J-aggregate dye layer (outer shell) [16]. The spacer layer used in the study was a cationic thiol which promoted the J-aggregation of anionic cyanine dyes onto the surface of the nanocomposite. The spectral line shape of these composites was dependent on the strength of the plasmon-exciton coupling between the metal core and the J-aggregate shell.

The metallic core composition and size, excitonic shell composition, degree of J-aggregate formation within the excitonic shell, and distance between the plasmonic core and excitonic shell are among the factors that play the most significant roles in controlling optical response. Metallic core particles and excitonic dyes of varying composition are readily available and selection is based on the intrinsic optical properties of the material. In terms of particle shape, a range of metallic core shapes such as spheres, rods, and platelets may be fabricated using well documented solution-based techniques [17–20]. However, spacer layer thickness and its impact on plasmon-exciton coupling in these nanoparticle systems have not been studied systematically. The spacer layer must serve the two-fold purpose of promoting the formation of a J-aggregate shell while also creating a distance, with specified length, between the metallic core and excitonic shell. To that end, we report the use of a variably thick polyelectrolyte spacer layer as a means of building multilayered plexcitonic nanoparticles and controlling plasmon-exciton distance. Specifically, we report the use of alternating cationic poly(diallyldimethyl ammonium chloride) (PDADMAC) and anionic poly(styrene sulfonate) (PSS) as a spacer layer between a silver core and a J-aggregate outer shell. The layer-by-layer self-assembly of oppositely charged polyelectrolytes has been used extensively as a means of coating and functionalizing colloidal particles [21,22]. The thickness of the polyelectrolyte spacer layer was controlled in this study by varying the number of PDADMAC/PSS layers that were adsorbed. The outer J-aggregate shell was formed by adsorbing the cationic form of PIC onto the outermost anionic PSS layer. A schematic of the double-shell structure is provided in Fig. 1(a). Figure 1(b) provides a schematic of the electrostatic adsorption of 1,1'-diethyl-2,2-cyanine (PIC) J-aggregates at the surface of a PDADMAC/PSS coated silver nanoparticle. The use of a polyelectrolyte spacer layer may be incorporated into a wide range of core-shell systems, regardless of geometry and composition. Therefore, this approach may be used as a means of studying plasmon-exciton coupling in a wide range of multilayered plexcitonic structures.
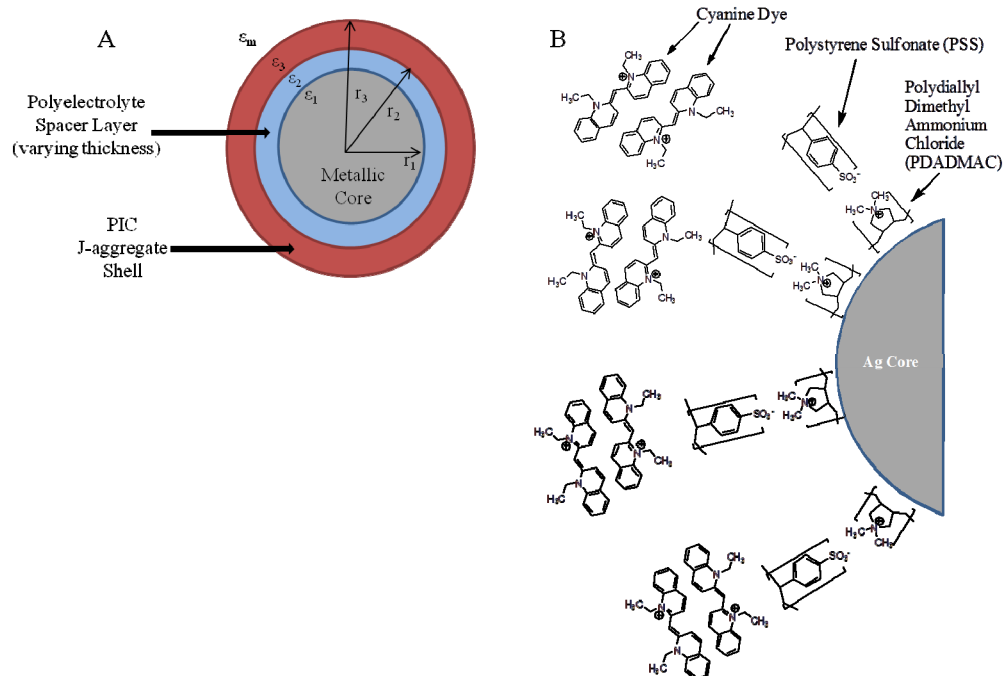
Fig. 1. Schematic of (A) a double-shell structure composed of a silver metallic core, a spacer layer consisting of alternating layers PDADMAC/PSS polyelectrolytes, and a 1,1'-diethyl-2,2'-cyanine iodide (PIC) exterior shell. The outer radius and dielectric function of individual layers are (R_i, ε_i, i = 1,2,…, n). The dielectric function of the medium is ε_m. (B) The electrostatic adsorption of (PIC) J-aggregates onto a silver core/polyelectrolyte spacer. Na$^+$, Cl$^-$, and I$^-$ ions are not drawn for clarity. Figures are not drawn to scale.

In order to explain the measured absorption features of the Ag/polyelectrolyte/PIC composite nanoparticles, Mie Theory and the Transfer Matrix Method were used to calculate the optical response of these multilayered nanospheres. Numerical simulations yielded good agreement with experimental results. Specifically, the impact of polyelectrolyte spacer layer thickness on the shift of the exciton frequency was elucidated. These results indicate that a polyelectrolyte spacer layer is a plausible means for tuning plasmon-exciton coupling in colloidal suspensions of multilayered plexcitonic nanoparticles.

2. Experimental methods

Silver nitrate, trisodium citrate tribasic dihydrate, sodium poly(styrene sulfonate) (PSS, MW ~70,000), poly(diallyldimethyl ammonium chloride) (PDADMAC, medium molecular weight 26062-79-3), sodium phosphate monobasic dihydrate, sodium phosphate dibasic dihydrate, and 1,1'-diethyl-2,2'-cyanine iodide were purchased from Sigma Aldrich (St. Louis, MO).

Silver nanoparticles were prepared using a modified procedure by Lee and Meisel in which Ag$^+$ ions are chemically reduced in aqueous solution [17]. Approximately 110 mg of AgNO$_3$ were dissolved in 400 mL deionized H$_2$O (18MΩ) and placed in a 1L 3-neck flask. A condenser tube (250 mm jacket length) was placed on the center neck of the flask to minimize evaporation losses. An addition funnel, containing 10 mL of 1% (wt/wt) trisodium citrate solution, was attached to a second neck of the flask. The solution was magnetically stirred and heated to 100°C using a heating jacket and temperature controller (Glass-Col, Terre Haute, IN) while refluxing. Once the boiling point was reached, the trisodium citrate solution was slowly added drop-wise. The mixture was heated and stirred for an additional hour at 100°C. The solution was then cooled to room temperature and stirring continued for an

additional hour. Assuming a 100% yield, the silver colloid had an approximate concentration of 0.3 mg/mL.

A standard solution of 1,1-diethyl-2,2'cyanine iodide (PIC) was prepared by dissolving 25 mg PIC in 100 mL phosphate buffer (pH = 6.0).

Silver core – polyelectrolyte shell nanoparticles were prepared by exposing the silver sol to supersaturated concentrations of polyelectrolytes. First, 10 mL Ag sol were transferred to a 50 mL polypropylene centrifuge tube. The sample was centrifuged at 4000 RPM for 15 minutes and the supernatant containing excess citrate was removed. 5 mL H_2O were then added to the tube followed by sonication. Next, 5 mL PDADMAC (1 mg/mL, 0.01 M NaCl) were added, and the suspension was vigorously mixed for 1 minute. The solution was allowed to stand for 30 minutes. Centrifugation (4000 RPM, 15 minutes) was used to remove the supernatant and excess polymer. Two cycles of a 10 mL water addition, followed by sonication, centrifugation, and supernatant removal were performed to ensure the removal of excess polymer. The same solution concentration and procedures used for the adsorption of PDADMAC were used for adsorption of additional polyelectrolyte layers (i.e. PSS, 1 mg/mL, 0.01 M NaCl). Combinations of 2, 4, and 6 polyelectrolyte layers, i.e. $(PDADMAC/PSS)_{1,2,3}$, were adsorbed onto the silver particles. The Ag core – polyelectrolyte shell nanoparticles were resuspended in 5 mL water with sonication.

For the in situ generation of a J-aggregate shell on the silver core – polyelectrolyte shell nanoparticles, the concentration of the Ag core - polyelectrolyte shell nanoparticle suspension was adjusted until absorbance measurements yielded an approximate absorbance of 0.5 to 1.5 absorbance units. This involved diluting 1 mL of the suspension to 25 mL with water. 3 mL of the diluted suspension were then placed in a 10 mm optical path quartz cuvette. 100 µL aliquots of PIC standard (0.25 mg/mL) were added to the cuvette, followed by mixing and immediate absorbance measurement.

Ag/polyelectrolyte/PIC composite nanoparticles were also prepared by exposing Ag core - polyelectrolyte shell nanoparticles to PIC for 24 hours. This involved placing 5 mL Ag core - polyelectrolyte shell nanoparticles in a 50 mL polypropylene centrifuge tube, follow by the addition of 5 mL of PIC standard. The samples sat for 24 hours to ensure adequate adsorption and aggregation of the dye onto the surface of the particles. The following day, the colloidal suspensions were centrifuged at 4000 RPM for 15 minutes, and the supernatant discarded for removal of excess PIC standard. The solid nanoparticles were washed with 10 mL water followed by sonication, centrifugation, and supernatant removal to ensure the removal of excess PIC. The particles were then resuspended in 5 mL water and sonicated. Finally, excessively large NPs were removed using a 0.22 µm Millex GP syringe filter. This procedure was repeated for each of the Ag/polyelectrolyte/PIC NP combinations.

All UV/Vis absorption spectra were measured in a quartz cuvette (10 mm optical path length) using a V-670 spectrophotometer (JASCO Co.). Spectra were measured from 190 nm to 800 nm. Transmission electron microscopy (TEM) images were observed in a FEI (Hillsboro, OR) Tecnai 12 TWIN TEM operating at 100kV. Samples were prepared by placing 5.0 µL of the particle solution onto a freshly ionized 300 copper mesh carbon coated/formvar grid. The samples were allowed to dry completely. Images were collected using an Olympus Soft Imaging System (Lakeland, CO) Megaview III digital camera. Figures were assembled in Adobe Photoshop using only linear adjustments in brightness and contrast. For the determination of zeta-potential, a Zetasizer Nano ZS (Malvern Instruments) was used to measure the electrophoretic mobilities of colloidal particles. The mobility µ was converted into a ζ-potential using the Smoluchowski relation ($\zeta = \mu\eta/\varepsilon$, where η is the viscosity of the solvent and ε is the permittivity of the solvent). The hydrodynamic radius was also determined using the Zetasizer Nano ZS instrument. This measurement is a dynamic light scattering technique.

3. Theoretical methods

In order to calculate the optical response of the Ag/polyelectrolyte/PIC nanocomposites, we generalize Mie theory to multilayer nanospheres via the Transfer Matrix Method [23–25]. For multilayer nanospheres, the electric field can be decomposed into orthogonal channels labeled by (σ, l), where σ takes TE or TM, and $l = 1, 2, 3,\dots$ [26–29]. The scattering and absorption cross-sections are the sum of contributions from each channel, and the extinction cross-section is the sum of scattering and absorption cross-sections:

$$\sigma_{sca} = \sum_{\sigma}\sum_{l=1}^{\infty} \frac{\lambda^2}{8\pi}(2l+1)\left|1-r_{\sigma,l}\right|^2 \tag{1}$$

$$\sigma_{sca} = \sum_{\sigma}\sum_{l=1}^{\infty} \frac{\lambda^2}{8\pi}(2l+1)\left|1-r_{\sigma,l}\right|^2 \quad \sigma_{ext} = \sigma_{sca} + \sigma_{abs} \tag{2}$$

In order to determine $r_{\sigma,l}$, we decompose the electric field inside each shell into incoming and outgoing spherical waves with coefficients (A_n, B_n). The coefficients of adjacent shells are connected by the transfer matrix of that interface, whose elements are determined by the boundary condition of TE or TM modes:

$$\begin{bmatrix} A_{i+1} \\ B_{i+1} \end{bmatrix} = M_{i+1,i} \begin{bmatrix} A_i \\ B_i \end{bmatrix} \tag{3}$$

The transfer matrix of the whole system can be calculated by combining the transfer matrices of individual interfaces:

$$\begin{bmatrix} A_{n+1} \\ B_{n+1} \end{bmatrix} = M_{n+1}, M_{n,n-1}\dots M_{3,2}, M_{2,1} \begin{bmatrix} A_1 \\ B_1 \end{bmatrix} = M \begin{bmatrix} A_1 \\ B_1 \end{bmatrix} \tag{4}$$

Since the second kind of spherical Bessel function is singular at the origin, we can set $A_1 = B_1 = 1$. Therefore,

$$r_1 = \frac{B_{n+1}}{A_{n+1}} = \frac{M_{21} + M_{22}}{M_{11} + M_{12}} \tag{5}$$

Incorporation of the appropriate dielectric constant for the aggregated form of PIC is required for the total cross-section calculations. We use a model that describes the red shifted energy of aggregate forms of cyanine dyes, in which [30]:

$$\varepsilon = \varepsilon_0 - 2V\cos\left(\frac{\pi}{N_c + 1}\right) \tag{6}$$

Here V is the nearest neighbor coupling energy, N_c is the number of coherently coupled molecules that make up the aggregate, and ε_0 is the frequency dependent dielectric constant of the monomer. Using this model for PIC, a red-shifted J-aggregate absorption peak at 575 nm is expected for aggregates composed of 14 or more dye molecules. This prediction is consistent with numerous experimental observations in which aggregated forms of PIC, both in solution and adsorbed onto surfaces, exhibit absorption at 575 nm [16,31]. Hence, 575 nm was taken as the excitation wavelength of the J-aggregate for the complex frequency-dependent dielectric function of the PIC J-aggregate, which was approximated using:

$$\varepsilon(\omega) = \varepsilon_0 + \frac{f\omega_0^2}{\omega_0^2 - \omega^2 - i\omega_0\gamma\omega} \tag{7}$$

Here, $\varepsilon_0 = \varepsilon_{medium} = 1.85$, ω_0 corresponds to the excitation frequency of the J-aggregate (corresponding to 575 nm), γ is the relaxation rate, and f represents the oscillator strength. Literature values for γ range from 0.01 to 0.02, and for f range from 0.01 to 1 [32].

4. Results and discussion

The citrate reduction method used in this study yielded silver core nanoparticles with an average particle size of 54.5 nm and a standard deviation of 9.8 nm. Figure 2(a) displays a TEM image of the silver nanoparticles. Most of the particles have a spherical shape with a relatively narrow size distribution, although a small amount of non-spherical particles are observed. Figure 2(b) displays the absorbance spectra of the silver colloid (blue curve) and the PIC standard (red curve). The silver colloid and PIC standard solutions are characterized by an absorption λ_{max} at 442 nm and 523 nm, respectively. Of particular note is the absence of the PIC J-aggregate peak, which is commonly observed at or near 575 nm. This observation is consistent with published data, as the concentration of the PIC standard in this solution is too low for the formation of the J-aggregate [16,31].
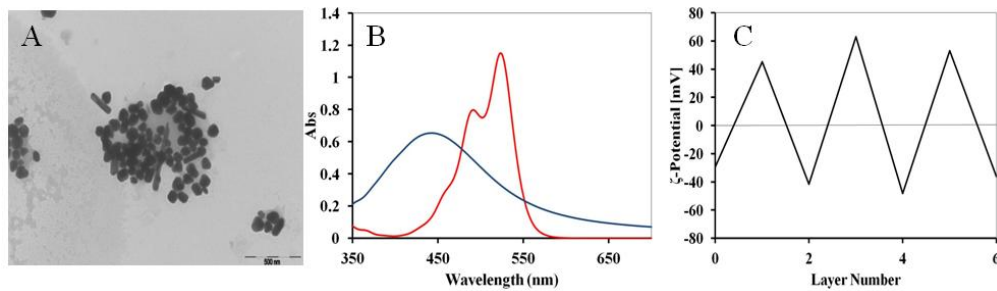

Fig. 2. (A) TEM image of silver nanoparticles fabricated using the citrate reduction method. (B) Experimental absorbance spectra of solutions containing 0.022 mg/mL silver sol (blue curve) and 0.023 mg/mL PIC (red curve). λ_{max} = 442 nm for the silver sol. λ_{max} = 523 nm for the PIC solution. (C) Zeta-potential as a function of layer number for silver particles coated with alternating layers of PDADMAC and PSS. Polyelectrolyte deposition of PDADMAC and PSS was performed in 0.01M NaCl.

Insertion of a polyelectrolyte layer between the Ag core and the cyanine dye outer shell was a central theme in this study. Specifically, our goal was to demonstrate the formation of the PIC J-aggregate on a silver core – polyelectrolyte shell composite nanoparticle. The layer-by-layer self assembly of polyelectrolytes on colloidal particles is an established technique for building stable and functionalized multilayers on nanoparticles. The irreversible electrostatic interaction between cationic and anionic polyelectrolyte layers aid in stabilizing these films. In our study, the sequential addition of PDADMAC and PSS, with PSS forming the outermost polyelectrolyte layer, was used to control the thickness of the polyelectrolyte layer and to render the outer surface of the particles with a negative charge. The negative surface charge promotes the adsorption and J-aggregation of the cationic PIC dye onto the surface of the particles. Figure 2(c) provides a summary of the ζ-potential measurements of Ag particles coated with sequential layers of PDADMAC and PSS. The ζ-potential alternates between positive and negative values for the sequential additions of PDADMAC and PSS, respectively.

Silver core – polyelectrolyte shell nanoparticles were exposed to PIC in a series of experiments. First, UV/Visible absorbance measurements of Ag core – polyelectrolyte shell colloids (0.013 mg/mL) were taken immediately after the addition of 100 μL increments of PIC standard, in order to determine if the PIC J-aggregate would form in situ. All in situ experiments were performed on Ag particles coated with one PDADMAC/PSS bi-layer. Figure 3 displays the absorbance spectra of these particles. As a control, the absorbance spectrum of Ag/PDADMAC/PSS was determined prior to the addition of PIC. The

absorbance spectrum of Ag/PDADMAC/PSS is characterized by a λ_{max} at 435 nm; compared to the absorbance spectra of the silver sol displayed in Fig. 2, it has a somewhat broader absorbance from 600 nm to 700 nm, possibly due to the slight agglomeration of silver core-polyelectrolyte shell nanoparticles. As PIC standard was incrementally added, a sharp peak near 570 nm is observed, indicative of J-aggregate formation. We note that the concentration of the PIC standard is too low to form J-aggregates in solution; therefore the observed J-aggregation of PIC must be promoted by the presence of the polyelectrolyte shell. J-aggregate peaks at 570 nm, 571 nm, and 571 nm were observed after the sequential addition of 100 µL, 200 µL, and 300 µL of PIC standard, respectively. Typically, when fully aggregated, the J-aggregate of PIC is characterized by an absorbance at 575 nm. Based on the theoretical model of the J-aggregate absorbance wavelength, we conclude that the PIC shell in this experiment is not in a fully aggregated form.
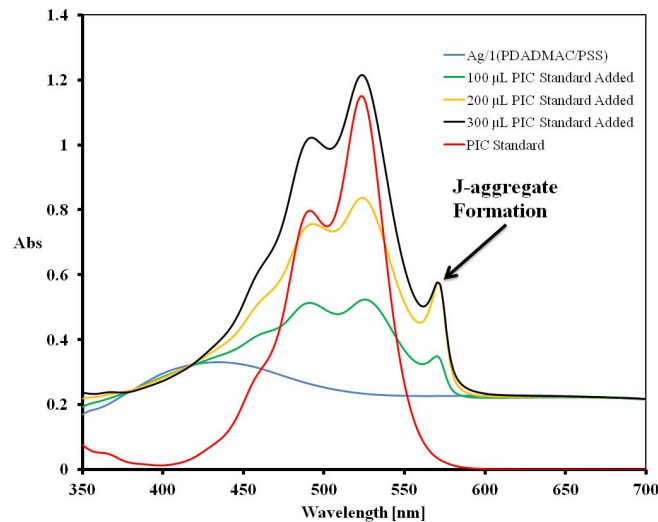

Fig. 3. Experimental absorbance spectra immediately following the sequential addition of PIC standard to a 3 mL colloidal suspension containing silver core-PDADMAC/PSS nanoparticles (0.013 mg/mL). 100 µL portions of a 0.23 mg/mL PIC standard solution were added to 3 mL of the suspension. The formation of the red-shifted J-aggregate peak was observed at 570 nm, 571 nm, and 571 nm upon addition of 100 µL, 200 µL, and 300 µL quantities of the PIC standard, respectively. For comparison, the absorbance spectra of the silver core/polyelectrolyte nanoparticles and PIC standard (0.023 mg/mL) are provided.

Next, we studied the impact of spacer layer thickness. This was achieved by adsorbing PIC to Ag/polyelectrolyte composite nanoparticles composed of 1 PDADMAC/PSS bi-layer, 2 PDADMAC/PSS bi-layers, and 3 PDADMAC/PSS bi-layers. In this set of experiments, formation of a fully aggregated PIC shell was promoted by exposing Ag/polyelectrolyte composite nanoparticle suspensions to PIC dye for 24 hours. A TEM image of the silver/polyelectrolyte/PIC nanoparticles is provided in Fig. 4(a). Figure 4(c) also displays the absorbance spectra of these experiments. The spectra is characterized by the formation of a red-shifted J-aggregate peak at 581 nm, 581 nm, and 579 nm for Ag particles coated with 1 (PDADMAC/PSS), 2 (PDADMAC/PSS), and 3 (PDADMAC/PSS) shells, respectively.
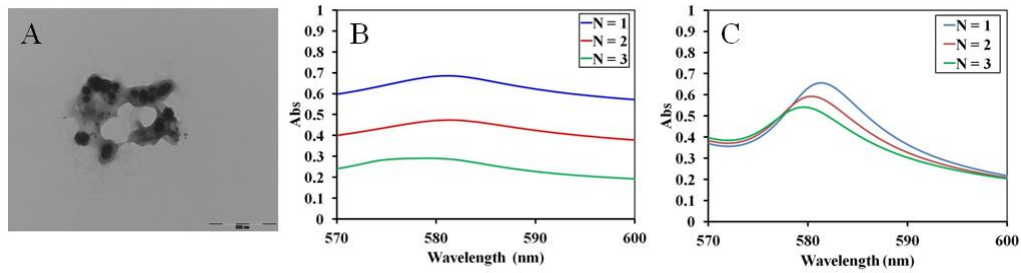
Fig. 4. (A) TEM image of silver/polyelectrolyte soaked in PIC for 24 hours. (B) Experimental absorbance spectra of PIC coated Ag core-polyelectrolyte shell nanoparticles, with varying polyelectrolyte layer thickness. 1 (PDADMAC/PSS) (blue curve), 2 (PDADMAC/PSS) (red curve), and 3 (PDADMAC/PSS) (green curve) correspond to 2, 4, and 6 alternating layers of PDADMAC and PSS, respectively. Formation of the red-shifted J-aggregate peak was observed at 581 nm, and 579 nm for the Ag/1(PDADMAC/PSS)/PIC, Ag/2(PDADMAC/PSS)/PIC, and Ag/3(PDADMAC/PSS)/PIC nanoparticles, respectively. (C) Simulated absorbance spectra for the impact of spacer layer thickness on the absorption wavelength of the J-aggregate peak. An oscillator strength (f) of 0.35 and a relaxation rate (γ) of 0.015 were assumed in the calculations.

The J-aggregate peaks were observed at wavelengths that were comparatively longer than what is commonly reported in the literature for PIC, i.e. 575 nm. Additionally, the J-aggregate peak wavelength was found to increase with decreasing spacer thickness. These results suggest that the PIC was fully, or close to fully aggregated, and that the plasmon-exciton interaction further red shifted the J-aggregate peak. This observation is consistent with the fact that plasmon-exciton interactions are enhanced as the distance between the J-aggregate shell and the Ag core particles is diminished.

Simulated absorbance spectra of Ag/(PDADMAC/PSS)/PIC nanoparticle composites were calculated in Fig. 4(c) in order to explain the main absorption features of the experimental data. For the dielectric constants, we used experimental frequency-dependent complex dielectric constant for the silver [33], literature values of 2.25 for PDADMAC and 2.56 for PSS [34], and Eq. (8) (with $f = 0.35$ and $\gamma = 0.015$) for the PIC J-aggregate. We assume a silver core of 54.5 nm (with SD = 9.8 nm), a J-aggregate dye outer shell of 5 nm, and a polyelectrolyte spacer of thickness 1 nm per bi-layer. This calculation is consistent for similar structures, in which the thickness of the polyelectrolyte bi-layers was determined to be 1.7 to 3.0 nm [21,34]. The simulation result in Fig. 4(c) was in qualitative agreement with the experimental absorbance spectra in Fig. 4 (b). Namely, the experimental and simulation results demonstrate the dependence of coupling strength and shift of the exciton frequency on spacer layer thickness. The red-shifted energy of the J-aggregate peak increases as the spacer layer thickness is minimized, i.e. the plasmon-exciton interaction is maximized. Discrepancies between the experimental and simulated results, in terms of J-aggregate peak shape, may be attributed to the fact that non-spherical and/or aggregated particles were not included in the simulated results.

5. Conclusion

Multilayered plexcitonic nanoparticles composed of an Ag core, polyelectrolyte spacer layer, and a PIC outer shell have been synthesized. The optical properties of the composite nanoparticles in aqueous solution were measured in the UV/Visible regions. Absorbance spectra of the colloidal nanoparticles indicate that PDADMAC/PSS spacer layers successfully promoted the J-aggregation of PIC. The in situ generation of the J-aggregate was observed when PIC standard was added directly to a colloidal suspension containing silver core – polyelectrolyte shell composite nanoparticles. The formation of the fully J-aggregated form was observed when PIC was exposed to a colloidal suspension of silver core – polyelectrolyte shell nanoparticles for 24 hours. The 24 hour study yielded a J-aggregate absorbance at 579-

581 nm, indicating the formation of a fully aggregated dye on the surface of the composites. The fully aggregated form of PIC is typically observed at 575nm. The additional red-shift in energy that was experimentally observed may be explained by the plasmon-exciton interaction between the silver core and the J-aggregate exterior. It is concluded that the use of oppositely charged polyelectrolytes is a valid approach for inducing the formation of J-aggregates on silver core-polyelectrolyte shell particles. Furthermore, polyelectrolyte spacer layers are a means of controlling the plasmon-exciton distance, which can ultimately be used to control the shift in exciton frequency. Finally, the ease with which polyelectrolyte layers are assembled onto colloidal nanoparticles of varying shape and composition, makes this technique suitable for building a wide range of plexcitonic particles.

Acknowledgments